ARTICLE NO. 80-4114

Flow in Streamwise Corners of Arbitrary Angle

W. H. Barclay* and A. H. Ridha†
University College London, England

A formulation of the problem posed by the flow along streamwise corners is presented. The corners are imagined to be formed by the abutment of two quarter-infinite planes along a side edge parallel to a uniform stream, and the treatment is general to any angle between the planes except the limiting angles 0 and 360 deg. The secondary shear layer, which exists in streamwise corner flows, is shown to exhibit a simple antisymmetric behavior for angles equidistant from 180 deg. This is explained in terms of the matching requirement between the potential flow and the outflow from the quasi-two-dimensional boundary layers adjacent to the corner layer. Numerical results are given in the form of velocity and wall shear stress distributions for corners of different angle. Agreement between these new results and available solutions for rectangular corners is excellent.

I. Introduction

THE flow in a rectangular streamwise corner formed by two semi-infinite rigid planes with coplanar leading edges has been treated in detail by Rubin et al.[1-3] More recently, Desai and Mangler[4] have published a method for dealing with corners of arbitrary angle, and Ghia[5] has reconsidered the rectangular corner. The solutions by Rubin and Ghia are in close agreement in most respects, but differ significantly from Desai and Mangler's results for the rectangular corner, particularly with regard to the secondary flow or crossflow.

A new formulation of the problem posed by the corner of arbitrary angle is presented herein, and the result is a set of equations that, when specialized to meet the rectangular corner situation, coincide with those obtained by Rubin.[1] Numerical results are given for the velocity and wall shear stress distributions for corner included angles ranging from 90 to 270 deg. The numerical method of solution adopted is rather similar to that used by Ghia, and the results for a rectangular corner are in excellent agreement with Ghia's solution for that case.

II. Analysis

A. Equations of Motion

The corner is formed by the abutment of two quarter-infinite planes joined along a side edge which is parallel to an infinite uniform stream of velocity U.

A coordinate system suitable for the present purpose is the x^1,x^2,x^3 system indicated in Fig. 1. The origin is in the symmetry plane at the leading edge. The x^1 axis is directed downstream. The x^2 and x^3 axes are normal to x^1 and lie, respectively, in the symmetry plane and in one of the joining quarter-infinite planes in order to form a right-handed oblique reference frame.

The disturbance caused by the corner to the otherwise uniform stream will result in a flow velocity vector which is a function of position and whose physical components in the x^1,x^2,x^3 directions we will denote by $v(1)$, $v(2)$, $v(3)$, respectively.

We will omit the routing but laborious procedure which shows that the governing equations, namely the Navier-Stokes and mass continuity equations, for steady incompressible flow can be written as

$$\frac{Dv(1)}{Dt} = -\frac{1}{\rho}\frac{\partial p}{\partial x^1} + \nu\overline{\nabla}^2 v(1) \tag{1}$$

$$\frac{D}{Dt}[v(2)+\sin\lambda v(3)] = -\frac{1}{\rho}\frac{\partial p}{\partial x^2} + \nu\overline{\nabla}^2[v(2)+\sin\lambda v(3)] \tag{2}$$

$$\frac{D}{Dt}[v(3)+\sin\lambda v(2)] = -\frac{1}{\rho}\frac{\partial p}{\partial x^3} + \nu\overline{\nabla}^2[v(3)+\sin\lambda v(2)] \tag{3}$$

$$\frac{\partial v(1)}{\partial x^1} + \frac{\partial v(2)}{\partial x^2} + \frac{\partial v(3)}{\partial x^3} = 0 \tag{4}$$

where

$$\frac{D}{Dt} \equiv v(1)\frac{\partial}{\partial x^1} + v(2)\frac{\partial}{\partial x^2} + v(3)\frac{\partial}{\partial x^3}$$

and

$$\overline{\nabla}^2 \equiv \frac{\partial^2}{(\partial x^1)^2} + \frac{1}{\cos^2\lambda}\left[\frac{\partial^2}{(\partial x^2)^2} - 2\sin\lambda\frac{\partial^2}{\partial x^2\partial x^3} + \frac{\partial^2}{(\partial x^3)^2}\right]$$

Attention will be confined to situations where the Reynolds number $Re \equiv 2Ux^1/\nu \gg 1$, in which ν is the kinematic viscosity. In such cases we assume the following series for the velocity components and the pressure:

$$v(1) = U\sum_{n=0}^{\infty} R_e^{-n/2} u_n(\xi^2,\xi^3) \tag{5a}$$

$$v(2) = U\sum_{n=1}^{\infty} R_e^{-n/2} v_n(\xi^2,\xi^3) \tag{5b}$$

$$v(3) = U\sum_{n=1}^{\infty} R_e^{-n/2} w_n(\xi^2,\xi^3) \tag{5c}$$

$$p = \rho U^2 \sum_{n=0}^{\infty} R_e^{-n/2} p_n(\xi^2,\xi^3) \tag{5d}$$

Received Dec. 4, 1978; revision received Feb. 12, 1980.

Index category: Boundary Layers and Convective Heat Transfer—Laminar.

*Lecturer, Dept. of Mechanical Engineering.
†Research Student, Dept. of Mechanical Engineering.

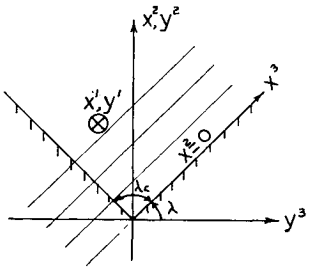

Fig. 1 Oblique (x^1,x^2,x^3) and Cartesian (y^1,y^2,y^3) coordinate systems.

where

$$\xi^2 \equiv R_e^{1/2} x^2/(2x^1) \quad \text{and} \quad \xi^3 \equiv R_e^{1/2} x^3/(2x^1)$$

Substitution from Eqs. (5) in Eqs. (1-4) and retaining only the most significant terms in each equation, yields the boundary-layer form of the equations appropriate to the problem. These are

$$-u_0[\xi^2 u_{0,2} + \xi^3 u_{0,3}] + v_1 u_{0,2} + w_1 u_{0,3} = \nabla^{*2} u_0 \tag{6}$$

$$-u_0[s_2 + \xi^2 s_{2,2} + \xi^3 s_{2,3}] + v_1 s_{2,2} + w_1 s_{2,3} = p_{2,2} + \nabla^{*2} s_2 \tag{7}$$

$$-u_0[s_3 + \xi^2 s_{3,2} + \xi^3 s_{3,3}] + v_1 s_{3,2} + w_1 s_{3,3} = p_{2,3} + \nabla^{*2} s_3 \tag{8}$$

$$-\xi^2 u_{0,2} - \xi^3 u_{0,3} + v_{1,2} + w_{1,3} = 0 \tag{9}$$

where

$$s_2 \equiv v_1 + \sin\lambda w_1$$

$$s_3 \equiv w_1 + \sin\lambda v_1$$

$$\nabla^{*2} \equiv \frac{1}{\cos^2\lambda}\left[\frac{\partial^2}{(\partial\xi^2)^2} - 2\sin\lambda\frac{\partial^2}{\partial\xi^2\partial\xi^3} + \frac{\partial^2}{(\partial\xi^3)^2}\right]$$

$$(\ )_{,2} \equiv \frac{\partial}{\partial\xi^2} \quad \text{and} \quad (\ )_{,3} \equiv \frac{\partial}{\partial\xi^3}$$

The simplifications consequent upon using Eqs. (5) are the absence from the boundary-layer equations of the operator corresponding to $\partial^2/(\partial x^1)^2$ which appears in the Navier-Stokes equations, and the vanishing of the pressure from the streamwise momentum Eq. (6).

The pressure is eliminated entirely on differentiating Eqs. (7) and (8) with respect to ξ^3 and ξ^2, respectively, and subtracting the results to get:

$$-u_0[2\omega_1 + \xi^2\omega_{1,2} + \xi^3\omega_{1,3}] + v_1\omega_{1,2} + w_1\omega_{1,3} + [v_{1,2} + w_{1,3}]\omega_1 + (u_{0,3}/\cos\lambda)[s_2 + \xi^2 s_{2,2} + \xi^3 s_{2,3}] - (u_{0,2}/\cos\lambda)[s_3 + \xi^2 s_{3,2} + \xi^3 s_{3,3}] = \nabla^{*2}\omega_1 \tag{10}$$

where

$$\omega_1 \equiv (1/\cos\lambda)[s_{3,2} - s_{2,3}] \tag{11}$$

Dropping the suffixes on u_0, v_1, w_1, and ω_1 for simplicity, Eqs. (6, 9, 10, and 11) can be cast in a more convenient form if v, w, and ω are expressed in terms of u and the new variables ϕ, ψ, and θ, defined as follows:

$$\left.\begin{aligned} &\phi = \cos\lambda(\xi^2 u - v), \quad \psi = \cos\lambda(\xi^2 u - w) \\ &\theta = (1/\cos\lambda)[(\xi^2\sin\lambda + \xi^3)u_{,2} - (\xi^2 + \xi^3\sin\lambda)u_{,3}] - \omega \end{aligned}\right\} \tag{12}$$

The resulting equations are

$$\nabla^2 u + \phi u_{,2} + \psi u_{,3} = 0 \tag{13}$$

$$\nabla^2\theta + \phi\theta_{,2} + \psi\theta_{,3} + 2u[c\theta + (\xi^2 + s\xi^3)u_{,3} - (s\xi^2 + \xi^3)u_{,2}] = 0 \tag{14}$$

$$\phi_{,2} + \psi_{,3} - 2cu = 0 \tag{15}$$

$$(s\phi_{,2} + \psi_{,2}) - (\phi_{,3} + s\psi_{,3}) - c^2\theta = 0 \tag{16}$$

where

$$\nabla^2 \equiv \frac{1}{\cos\lambda}\left[\frac{\partial^2}{(\partial\xi^2)^2} - 2\sin\lambda\frac{\partial^2}{\partial\xi^2\partial\xi^3} + \frac{\partial^2}{(\partial\xi^3)^2}\right]$$

and s and c are abbreviations for $\sin\lambda$ and $\cos\lambda$, respectively. Equations (13-16) are to be solved throughout the region $0 \le \xi^2, \xi^3 \le \infty$ subject to the boundary conditions derived in the following section.

B. Boundary Conditions

1. Conditions on the Wall, $\xi^2 = 0$

To satisfy the no-slip condition at solid boundaries, we must have

$$\xi^2 = 0; \quad u = v = w = 0 \tag{17a}$$

whereupon

$$\phi = \psi = 0 \tag{17b}$$

and from the defining Eq. (16)

$$\theta = (1/c^2)\psi_{,2} \tag{17c}$$

since $\phi_{,2} = 0$ from continuity Eq. (15).

2. Conditions on the Symmetry Plane, $\xi^3 = 0$

Return for a moment to the Cartesian coordinate frame (y^1,y^2,y^3) shown in Fig. 1, and let $v^*(1)$, $v^*(2)$, $v^*(3)$ be the velocity components in the y^1,y^2,y^3 directions, respectively. It is evident that $v^*(1)$ and $v^*(2)$ are symmetric with respect to the symmetry plane $y^3 = 0$, whereas $v^*(3)$ and the streamwise vorticity $\omega^*(1)$ are antisymmetric, i.e.,

$$y^3 = 0; \quad \frac{\partial v^*(1)}{\partial y^3} = \frac{\partial v^*(2)}{\partial y^3} = v^*(3) = \omega^*(1) = 0 \tag{18}$$

These are the conditions to be satisfied at the symmetry plane, and in terms of the variables used in Eqs. (13-16), they become

$$\xi^3 = 0; \quad u_{,3} - su_{,2} = 0, \quad \phi_{,3} - s\phi_{,2} + s\psi_{,3} = 0, \quad \psi = \theta = 0 \tag{19}$$

These results remind us that it is not necessary, if sometimes convenient, that the coordinate system be symmetric with respect to the physical plane of symmetry. Equations (19) represent the condition that the flow is symmetrical about the $y^3 = 0$ plane, and provided the condition is satisfied, the precise form of the continuous coordinate system in which it is expressed is, to that extent, unimportant.

3. Conditions as $\xi^2 \to \infty$

As $\xi^2 \to \infty$, the streamwise velocity component approaches its freestream value and the vorticity vanishes, i.e.,

$$\xi^2 \to \infty; \quad u \sim 1, \quad \theta \sim 0 \quad \text{[see Eq. (12)]} \tag{20}$$

The conditions on ϕ and ψ as $\xi^2 \to \infty$ are less obvious but are none the less simply obtained by observing that, in the

absence of a streamwise pressure gradient, the crossflow velocity vector must be invariant [to $O(Re^{-1/2})$] with respect to ξ^2 in this limit. The velocity components, therefore, must also be independent of ξ^2 as $\xi^2 \to \infty$. The variation in v and ω can then be found as follows:

The continuity equation and the vorticity definition in terms of the velocity components u,v,w are

$$-\xi^2 u_{,2} - \xi^3 u_{,3} + v_{,2} + w_{,3} = 0 \tag{21a}$$

$$-\omega c + (w+sv)_{,2} - (v+sw)_{,3} = 0 \tag{21b}$$

When $\xi^2 \to \infty$,

$$u_{,2} = u_{,3} = v_{,2} = w_{,2} = \omega = 0$$

then

$$w_{,3} = 0 \quad \text{and} \quad (v+sw)_{,3} = 0$$

Therefore,

$$\left.\begin{aligned} &w = \text{const} \\ &= 0 \text{ since } \psi = 0 \text{ at } \xi^3 = 0 \text{ [Eqs. (19) and (12)]} \\ &\text{and} \\ &v = \text{const} = \beta \end{aligned}\right\} \tag{22}$$

The value of β will be determined by the need to match with the outflow from the boundary layer where $\xi^3 \to \infty$ discussed below.

The boundary conditions for ϕ and ψ now follow from Eqs. (12), (20), and (22) as

$$\xi^2 \to \infty;\ \phi \to c(\xi^2 - \beta),\ \psi \to c\xi^3 \tag{23}$$

4. Conditions as $\xi^3 \to \infty$

Since θ and ψ are unbounded when $\xi^3 \to \infty$ [see Eq. (12)], it would be incorrect to set derivatives with respect to ξ^3 equal to zero in Eqs. (13-16) in order to obtain the equations governing the flow at large ξ^3. Instead, we formally assume that when ξ^3 is large, the dependent variables can be represented by‡

$$u \sim \sum_{n=0}^{\infty} (\xi^3)^{-n} u_n(\xi^2), \quad \phi \sim \sum_{n=0}^{\infty} (\xi^3)^{-n} \phi_n(\xi^2) \tag{24a}$$

$$\theta \sim \sum_{n=0}^{\infty} (\xi^3)^{-n+1} \theta_n(\xi^2), \quad \psi \sim \sum_{n=0}^{\infty} (\xi^3)^{-n+1} \psi_n(\xi^2) \tag{24b}$$

complemented by

$$v \sim \sum_{n=0}^{\infty} (\xi^3)^{-n+1} v_n(\xi^2), \quad w \sim \sum_{n=0}^{\infty} (\xi^3)^{-n+1} w_n(\xi^2) \tag{25}$$

Placing series (24) into Eqs. (13-16), and collecting terms of equal order in ξ^3, gives the following equations for the leading terms

$$u_0'' + c\phi_0 u_0' = 0 \tag{26a}$$

$$\theta_0'' + c\phi_0\theta_0' + c\psi_0\theta_0 + 2cu_0(c\theta_0 - u_0') = 0 \tag{26b}$$

$$\phi_0' + \psi_0 - 2cu_0 = 0 \tag{26c}$$

$$c^2\theta_0 - \psi_0' = 0 \tag{26d}$$

‡The asymptotic forms [Eqs. (24)] are similar to those used by Pal and Rubin.[2] In both Eqs. (24) and (25) we employ a notation like that already used in Eq. (5), in the belief that these will not be confused. It is a matter of temporary expedience only.

where a dash denotes differentiation with respect to ξ^2.

In addition to Eqs. (26), we also have the complementary equations

$$\phi_0 = c(\xi^2 u_0 - v_0), \quad \psi_0 = cu_0 \tag{27}$$

on substituting Eqs. (24) and (25) into Eq. (12).

The solutions of Eqs. (26) are

$$u_0 = f', \quad \phi_0 = cf, \quad \theta_0 = f''/c, \quad \psi_0 = cf' \tag{28a}$$

where f is the solution of

$$f''' + c^2 ff'' = 0 \tag{28b}$$

subject to

$$f(0) = f'(0) = 0 \quad \text{and} \quad f'(\infty) = 1 \tag{28c}$$

The problem for f is just the Blasius flat-plate boundary-layer problem in oblique coordinates. The details of its solution will be omitted here (see Ref. 7, p. 223).

The equations for ϕ_1 and u_1 are

$$(1/c^2)\phi_1''' + f\phi_1'' - f'\phi_1' + 2f''\phi_1 = 0, \quad \phi_1' - 2cu_1 = 0$$

together with the boundary conditions

$$\xi^2 = 0;\ \ \phi_1 = 0, \quad \xi^2 \to \infty;\ \ \phi_1 = 0$$

The only solution is $\phi_1 = u_1 = 0$.

Incorporating all of the above results, the equations for θ_1 and ψ_1 are

$$\theta_1'' + c\phi_0\theta_1' + 2c^2 f'\theta_1 + c\theta_0\psi_1 = 2(s/c)f''' + 2sc\xi^2 f'f'' \tag{29}$$

$$c^2\theta_1 - \psi_1' = 0 \tag{30}$$

Putting $\theta_1 = (1/c^2)\psi_1'$ from Eq. (30) into Eq. (29) gives

$$(1/c^2)\psi_1''' + f\psi_1'' + 2f'\psi_1' + f''\psi_1 = 2(s/c)f''' + 2sc\xi^2 f'f'' \tag{31}$$

with the boundary conditions

$$\xi^2 = 0;\ \ \psi_1 = 0, \quad \xi^2 \to \infty;\ \ \psi_1 = 0$$

Equation (31) has the solution

$$\psi_1 = -sc^3\beta f'' \int_0^{\xi^2} \frac{\eta - \beta}{f''(\eta)}\, d\eta + sc(\xi^2 f' - f) \tag{32}$$

and, therefore, from Eq. (30)

$$\theta_1 = -sc\beta\left[f''' \int_0^{\xi^2} \frac{\eta - \beta}{f''(\eta)}\, d\eta + \xi^2 - \beta\right] + \frac{s}{c}\xi^2 f'' \tag{33}$$

Continuing to the case where $n = 2$, with some algebra it can be shown that

$$(1/c^2)w_2''' + (fw_2')' = 0, \ \ \xi^2 = 0;\ \ w_2 = 0, \ \ \xi^2 \to \infty;\ \ w_2 = 0 \tag{34}$$

This homogeneous system has as its only solution, $w_2 = 0$. Similarly, it is found that $u_2 = \phi_2 = \theta_2 = 0$. In general, $u_n = \phi_n = \psi_n = \theta_n = 0$ for $n \geq 2$ and, consequently, $v_n = w_n = 0$, $n \geq 2$.

Collecting the results of this section for convenience, we have for the boundary conditions as $\xi^3 \to \infty$,

$$u = f' \tag{35a}$$

$$\theta = \frac{1}{c}\xi^3 f'' - cs\beta\left[f''' \int_0^{\xi^2} \frac{\eta - \beta}{f''(\eta)}\, d\eta + \xi^2 - \beta\right] + \frac{s}{c}\xi^2 f'' \tag{35b}$$

$$\phi = cf \tag{35c}$$

$$\psi = c\xi^3 f' - c^3 s\beta f'' \int_0^{\xi^2} \frac{\eta-\beta}{f''(\eta)}\,d\eta + sc(\xi^2 f' - f) \tag{35d}$$

The boundary-layer flow along a corner is, therefore, completely specified by Eqs. (13-16) and boundary conditions (17), (19), (20), (23), and (35).

Desai and Mangler,[4] in their analysis of the present problem, arrived at a set of boundary conditions different from those given above. Part of the difference arises from the implicit assumption by Desai and Mangler that the flow at $\xi^3 \to \infty$ corresponds exactly to that for a semi-infinite flat plate, i.e., $u = f'$ and the crossflow velocity vector of magnitude $(Uv/2x')^{1/2}(\xi^2 f' - f)$ is normal to the wall. They also used weaker conditions on ϕ and ψ at $\xi^2 \to \infty$, wherein only the gradients $\phi_{,2}$ and $\psi_{,2}$ are specified, whereas by the method of (3) above we are able to prescribe the values of ϕ and ψ explicitly in this limit. These defects in the boundary conditions are sufficient to account for the unsatisfactory agreement referred to in Sec. I between the numerical results obtained by Desai and Mangler and those due to Rubin and Grossman[3] and Ghia.[5]

III. Asymptotic Crossflow Velocity

From the definition of ψ [Eq. (12)] and the results of Sec. II (4), the crossflow velocity w at $\xi^3 \to \infty$ is found to be

$$w = sc^2\beta f'' \int_0^{\xi^2} \frac{\eta-\beta}{f''(\eta)}\,d\eta - s(\xi^2 f' - f) \tag{36}$$

This result is a generalization of that derived in Ref. 1 which concerns the rectangular corner. It can be shown to be so by referring Eq. (36) to an orthogonal Cartesian coordinate system where ξ^2 of the present system is replaced by a similarly stretched coordinate η normal to ξ^3. If $\hat{v}$ and $\hat{w}$ are, respectively, the components of the crossflow velocity vector normal and parallel to the wall, then

$$\eta = \xi^2\cos\lambda, \quad \hat{v} = v\cos\lambda, \quad \hat{w} = w + v\sin\lambda \tag{37}$$

Substituting from Eqs. (27), (35), and (36) in Eq. (37) gives

$$\hat{v} = \eta\dot{F}(\eta) - F(\eta)$$

$$\hat{w} = \beta_0\tan\lambda\ddot{F}(\eta)\int_0^{\eta} \frac{\tau-\beta_0}{\ddot{F}(\tau)}\,d\tau \tag{38}$$

where $F(\eta)$ is the Blasius function in the new coordinate system, a dot denotes differentiation with respect to η, and β_0 is given by

$$\beta_0 = \lim_{\eta\to\infty}(\eta\dot{F}(\eta) - F(\eta))$$

or in terms of the ξ^i system by

$$\beta_0 = \beta\cos\lambda$$

For a 90 deg corner $\lambda = 45$ deg and Eq. (38) then gives the same crossflow velocity as obtained in Ref. 1.

From Eq. (38), we may write $\hat{w} = \beta_0\tan\lambda\dot{H}(\eta)$, where $\dot{H}(\eta)$ is a function determined by Rubin.[1] β_0 and $\dot{H}(\eta)$ are independent of λ; therefore, $\hat{w}$ varies as $\tan\lambda$. For example, the distribution of $\hat{w}$ for $\lambda = -45$ deg is a mirror image of that for $\lambda = +45$ deg. This remarkable antisymmetry in $\hat{w}$ with respect to λ is explained when we understand the controlling influence of the potential flow on the boundary layers.

The corner layer extends over the region $0 \le \xi^2$, $|\xi^3| \le \infty$, which, in terms of the unstretched physical coordinates, is the domain x^1 fixed, $x^2 = 0^+$, $|x^3| = 0^+$ $(R_e \to \infty)$, and matching between the viscous region of the corner flow and the potential flow is to be effected in this vicinity. The potential crossflow controlling the corner layer is the potential solution for the region $x^2 = 0^+$, $|x^3| < 0^+$ which, in the limit x^1 fixed, $R_e \to \infty$, is the vector at $x^2 = 0^+$, $x^3 = 0$ and which necessarily lies in the symmetry plane. This vector must have the component $\beta_0 Re^{-1/2}$ normal to the wall in order to match with the outflow $\beta_0 Re^{-1/2}$ from the boundary layer at $x^2 = 0^+$, $|x^3| > 0^+$ and, therefore, it has the magnitude $\beta_0 Re^{-1/2}/\cos\lambda$ $(\lambda \pm 90$ deg). Consequently, its component parallel to the wall is $\beta_0 Re^{-1/2}\tan\lambda$ and this gives rise to a secondary shear layer for which Eq. (38) is the solution. These matters are illustrated in Fig. 2.

This method could have been used to arrive at the asymptotic boundary conditions for the corner layer at $\xi^2 \to \infty$ and $\xi^3 \to \infty$ directly on knowing $\dot{H}(\eta)$.

IV. Method of Solution

In arriving at the boundary-layer equations for the corner flow and their boundary conditions, there has been no hint of any inconvenient behavior in the flow variables when ξ^2 or ξ^3 is large. Specifically, the vanishing of the algebraic terms in the velocity components [Eqs. (24) and (25)] seems to imply an exponential decay into the quasi-two-dimensional boundary layer at large ξ^3. This would normally be an eminently satisfactory result, since it means that boundary conditions could be applied at moderate values of the coordinates. Satisfactory that is, were it not for the fact that the analysis by Pal and Rubin[2] and the solutions by Rubin and Grossman[3] and Ghia[6] exhibit an algebraic decay that we have been seeking. Evidently the different coordinate systems used play a part in this seemingly paradoxical result and their role is illustrated in Fig. 3. The algebraically decaying region is qualitatively of the form shown, and from this we can infer the consequences for the expansions (24) and (25) in Rubin's coordinates and in the present system. In Rubin's system, one boundary is on the symmetry line and the condition there must acknowledge the algebraic decay; whereas in the present coordinates the equations to be solved on any ξ^3 line permit the use of a boundary condition in the potential region. Since the assumed series provides no other mechanism for bringing out the algebraic decay, the phenomenon is missed entirely and the results of the series are therefore only valid strictly at

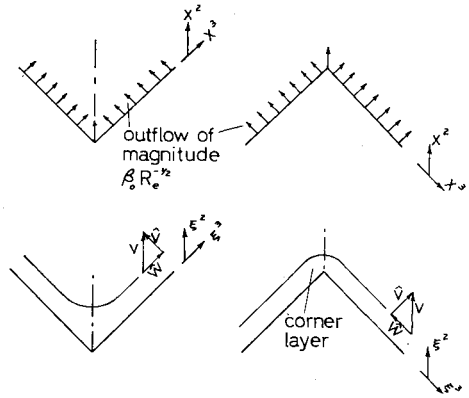

Fig. 2 Antisymmetry in $\hat{w}(\lambda)$. The corner layer, visible in the ξ^2,ξ^3 plane, shrinks to the vicinity of the point (0,0) in the x^2,x^3 plane.

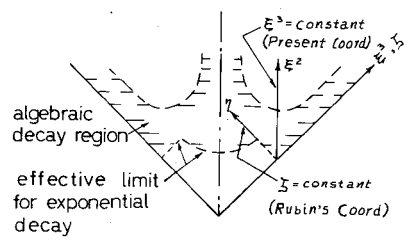

Fig. 3 Importance of the coordinate system in detecting algebraic decay. Equations solved in planes ξ^3 large are subject to boundary conditions in the potential flow region and algebraic decay may be missed.

$\xi^3 \to \infty$. In contrast, the practicalities of computing limit the integration domain to something less than $\xi^3 = 20$ which is likely to be well inside the decay region. Clearly, an analogous situation also exists with regard to the ξ^2 coordinate.

Two ways out of the difficulty are available. One is to seek a series that better represents the flow behavior at large values of the coordinates. The most profitable technique, however, is to employ a mapping scheme which transforms the quarter-infinite region $0 \le \xi^2, \xi^3 \le \infty$ into the finite region $0 \le \eta, \zeta \le k$ where k is a finite constant fixed by the chosen transformations $\eta(\xi^2), \zeta(\xi^3)$. The mapping approach was used by Ghia,[6] and Desai and Mangler[4] and is preferred by the present writers since it avoids the need to study the nature of the decay into the "side-edge" boundary layers and potential region. However, we shall use it in an incomplete form. Our particular interest is in the streamwise velocity component u and this, together with the streamwise vorticity component, are known to asymptote to their potential flow values exponentially fast but considerably more slowly into the adjacent boundary layers. Therefore, it is likely that the boundary conditions at $\xi^2 \to \infty$ can be replaced (as is commonly done in boundary-layer problems) by imposing the same conditions at a moderate value of ξ^2 with little effect on the streamwise velocity. On this argument the ξ^2 coordinate was left unaltered, a decision justified by the numerical results obtained.

With regard to the ξ^3 direction, all of the flow variables decay algebraically to their boundary-layer values and this must be allowed for. Consequently, the range $0 \le \xi^3 < \infty$ was transformed to $0 \le \zeta < 1/b$ on defining the variable ζ by

$$\zeta = \frac{\xi^3}{a + b\xi^3} \tag{39}$$

This transformation maps equal intervals in ζ into unequal intervals in ξ^3 with the step size in ξ^3-growing as ζ increases. It has the desirable effect of increasing the resolution near $\xi^3 = 0$, where changes with respect to ξ^3 are expected to be most rapid. In this vicinity, the interval in ξ^3 is approximately $a\zeta$.

The variables ψ and θ are unbounded as $\xi^3 \to \infty$, but this inconvenience is avoided by replacing ψ and θ with the new variables $\bar{\psi}$ and $\bar{\theta}$, defined by

$$\psi = \bar{\psi} + c\xi^3 f' \quad \text{and} \quad \theta = \bar{\theta} + (1/c)\xi^3 f'' \tag{40}$$

Before introducing the new variables, Eqs. (15) and (16) are converted to elliptic Poisson-like forms better suited to numerical treatment by relaxation methods. This is effected by differentiating both equations with respect to ξ^2 and ξ^3, which with some algebra leads to

$$\phi_{,22} + \phi_{,33} - s\phi_{,23} + s\psi_{,33} + c^2\theta_{,3} - 2cu_{,2} = 0 \tag{41}$$

$$\psi_{,22} + \psi_{,33} - s\psi_{,23} + s\phi_{,22} - c^2\theta_{,2} - 2cu_{,3} = 0 \tag{42}$$

The equations to be solved are now Eqs. (13, 14, 41, and 42) which, in terms of the new variables, become

$$\nabla^{*2} u + \phi u_{,2} + Du_{,\zeta} = 0 \tag{43a}$$

$$\nabla^{*2}\bar{\theta} + \phi\bar{\theta}_{,2} + D\bar{\theta}_{,\zeta} + 2u[c\bar{\theta} + \zeta_1(\xi^2 + s\xi^3)u_{,\zeta} - (s\xi^2 + \xi^3)u_{,2} + \xi^3 f''] + (1/c)f''\bar{\psi} + (1/c)\xi^3 f'''\phi + (1/c^2)\xi^3 f''' - 2(s/c^2)f''' + \xi^3 f' f'' = 0 \tag{43b}$$

$$\phi_{,22} + \zeta_1^2\phi_{,\zeta\zeta} - s\zeta_1\phi_{,2\zeta} + \zeta_2\phi_{,\zeta} + s\zeta_1^2\bar{\psi}_{,\zeta\zeta} + s\zeta_2\bar{\psi}_{,\zeta} - 2cu_{,2} + \zeta_1 c^2\bar{\theta}_{,\zeta} + cf'' = 0 \tag{43c}$$

$$\bar{\psi}_{,22} + \zeta_1^2\bar{\psi}_{,\zeta\zeta} - s\zeta_1\bar{\psi}_{,2\zeta} + \zeta_2\bar{\psi}_{,\zeta} + s\phi_{,22} - 2c\zeta_1 u_{,\zeta} - c^2\bar{\theta}_{,2} + \zeta_2\bar{\psi}_{,\zeta} - scf'' = 0 \tag{43d}$$

where

$$\zeta_1 \equiv \frac{d\zeta}{d\xi^3}, \quad \zeta_2 \equiv \frac{d^2\zeta}{(d\xi^3)^2}, \quad u_{,\zeta} \equiv \frac{\partial u}{\partial \zeta}, \quad \bar{\theta}_{,\zeta} \equiv \frac{\partial \bar{\theta}}{\partial \zeta}$$

$$\nabla^{*2} \equiv \frac{1}{c}\left[\frac{\partial^2}{(\partial\xi^2)^2} - 2s\zeta_1\frac{\partial^2}{\partial\xi^2\partial\zeta} + \zeta_1^2\frac{\partial^2}{\partial\zeta^2}\right]$$

$$D \equiv \zeta_1(\bar{\psi} + \xi^3 cf') + \zeta_2/c$$

The boundary conditions are now

$$\xi^2 = 0; \quad u = \phi = \bar{\psi} = 0, \quad \bar{\theta} - \frac{1}{c^2}\bar{\psi}_{,2} = 0 \tag{44a}$$

$$\zeta = 0 \ (\xi^3 = 0) \quad \begin{cases} \zeta_1 u_{,\zeta} - su_{,2} = 0, & \bar{\theta} = \bar{\psi} = 0 \\ \zeta_1\phi_{,\zeta} - s\phi_{,2} + s\zeta_1\bar{\psi}_{,\zeta} + scf' = 0 \end{cases} \tag{44b}$$

$$\xi^2 \to \infty \quad \begin{cases} u \sim 1, & \bar{\theta} \sim 0 \\ \phi \to c(\xi^2 - \beta), & \bar{\psi} \to 0 \end{cases} \tag{44c}$$

$$\zeta = \frac{1}{b} \ (\xi^3 = \infty) \quad \begin{cases} u = f', \quad \phi = cf \\ \bar{\theta} = -sc\beta\left[f'''\int_0^{\xi^2}\frac{\eta - \beta}{f''(\eta)}\,d\eta + \xi^2 - \beta\right] + \frac{s}{c}\xi^2 f'' \\ \bar{\psi} = -sc^3\beta f''\int_0^{\xi^2}\frac{\eta - \beta}{f''(\eta)}\,d\eta + sc(\xi^2 f' - f) \end{cases} \tag{44d}$$

Equations (43) subject to Eqs. (44) were solved numerically by the Gauss-Seidel iterative method. There is freedom to choose the constants a and b in Eq. (39), the outer limit on ξ^2 ($\equiv \xi^2_{\max}$, for instance), and the mesh interval h. The choice was made on the basis that small variations about the chosen values should have a negligible effect on the solution. After some experimental computations the following were adopted for all subsequent calculations:

$$a = 0.5, \ \zeta = \zeta_{\max} = 14.4 (b = 0.0694), \ \xi^2_{\max} = 16.0, \ h = 0.4$$

The solution was deemed satisfactory when the difference in the values of $u, \bar{\theta}, \phi$, and $\bar{\psi}$ from successive iterations was less than 0.0001 at every mesh point.

V. Numerical Results

A. Streamwise Velocity

The results are illustrated in Figs. 4-12. The natural first step in considering the results is to compare them with what is believed to be the most accurate solutions available for the rectangular corner.[3,5] The streamwise velocity profile in the symmetry plane is the characteristic profile of the flow and this is shown in Fig. 4, along with those from the solutions by Rubin and Grossman[3] and Ghia.[5,6] In addition, the Blasius profile is included to afford some reference against which to measure the effect of the corner on the one hand and the differences among the symmetry plane results on the other. The isovels for u, as seen in planes $x' =$ constant, are shown in Fig. 5, also with those from Refs. 3 and 6.

The agreement of the new results with those by Ghia is excellent and with regard to the streamwise velocity distribution at least, is a vindication of the decision not to introduce a variably stretched coordinate in the ξ^2 direction.

To illustrate the effect of a change of angle on the streamwise velocity distribution, the isovels of u for a 270 deg corner are shown in Fig. 6 for comparison with Fig. 5.

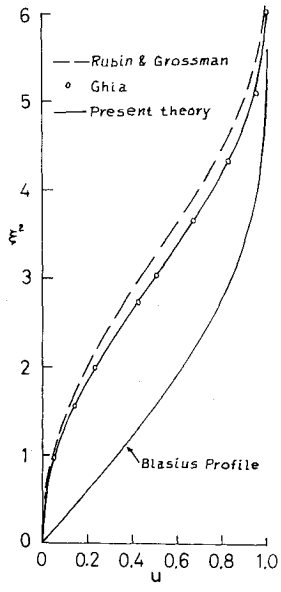

Fig. 4 Streamwise velocity u in the symmetry plane of a rectangular corner.

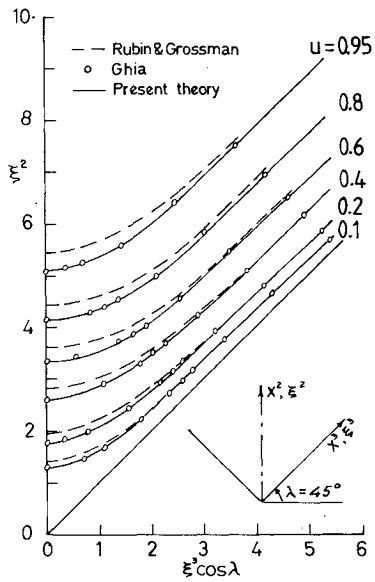

Fig. 5 Streamwise isovels in a rectangular corner.

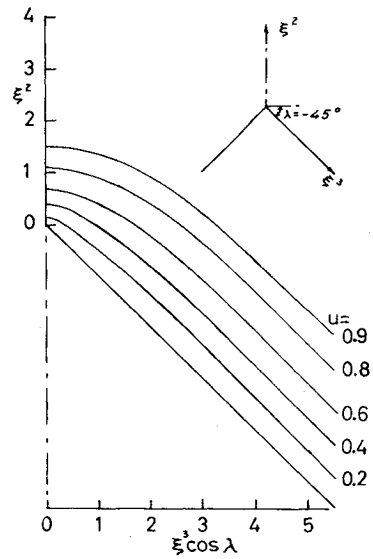

Fig. 6 Streamwise isovels in a 270 deg corner.

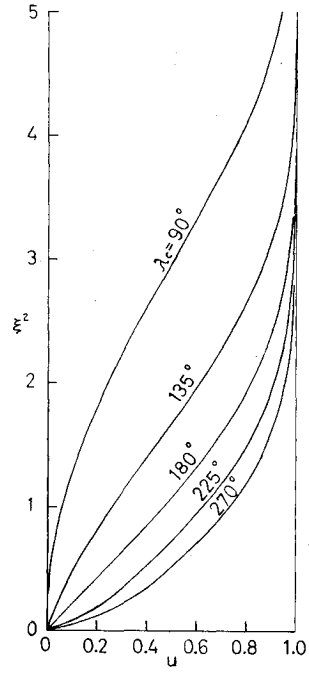

Fig. 7 Streamwise velocity u in the symmetry plane for different corner angles.

Complementing these in Fig. 7, which shows the effect of corner angle on the streamwise velocity profile in the symmetry plane for angles in the range 90-270 deg. In all the figures, the streamwise velocity behaves in a regular and expected fashion, the thickness (and the rate of thickening) of the corner layer as measured in the symmetry plane becoming greater as the corner angle is reduced. The separation-like character of the streamwise velocity profile has been pointed out many times before in the literature on the rectangular corner. This character is typical for corners of all angles less than 180 deg, but is absent from the profiles corresponding to larger angles.

B. Crossflow

Turning to the crossflow, the agreement with the solutions in Refs. 3 and 6 is gaged by comparing in Fig. 8 the component $v^*(2)$ in the symmetry plane from each source. The agreement is good among all the results up to $\xi^2 = 5$ approximately, but thereafter the different method adopted in each case for treating the problem at large ξ^2 is the likely reason for the differences seen in the results. In every case, however, the asymptotic behavior of $v^*(2)$ is algebraic. It is to be noted that at $\xi^2 = 5$, $u(\approx 0.94)$ is already near its asymptotic limit (see Fig. 4) and is practically unaffected by the

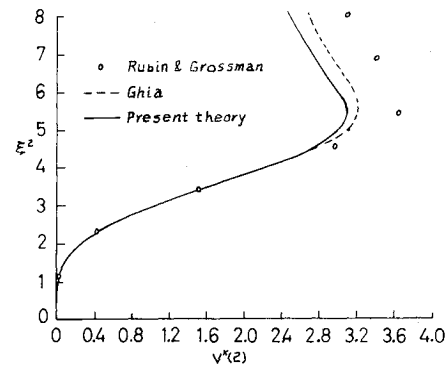

Fig. 8 Cartesian crossflow velocity component $v^*(2)$ in the symmetry plane of a rectangular corner.

algebraic behavior of the crossflow at larger ξ^2. Figure 9 shows the symmetry plane profiles of $v^*(2)$ for corner angles λ_c in the range of 90-270 deg. In general, for any given angle the crossflow throughout the corner behaves in a rather complex fashion and its description is assisted by the

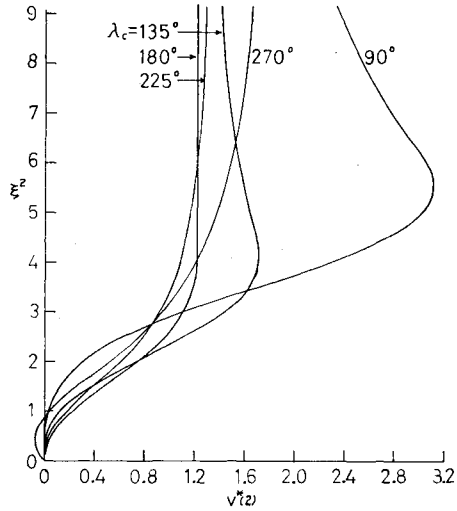

Fig. 9 Cartesian crossflow velocity component $v^*(2)$ in the symmetry plane for different corner angles. Note that the profiles for the two corners of angles $\lambda_c = 180$ deg $\pm 2|\lambda|$ deg asymptote to the same limit as $\xi^2 \to \infty$.

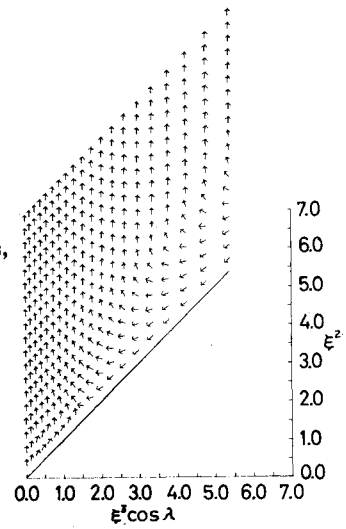

Fig. 10 Crossflow directions, $\lambda_c = 90$ deg.

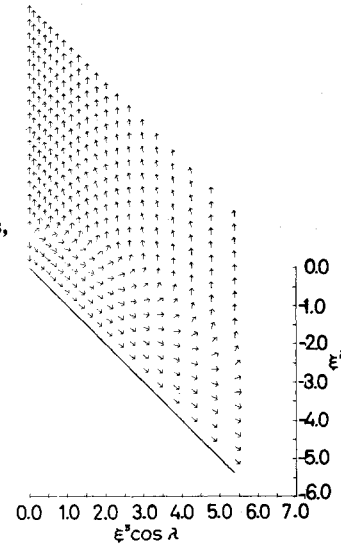

Fig. 11 Crossflow directions, $\lambda_c = 270$ deg.

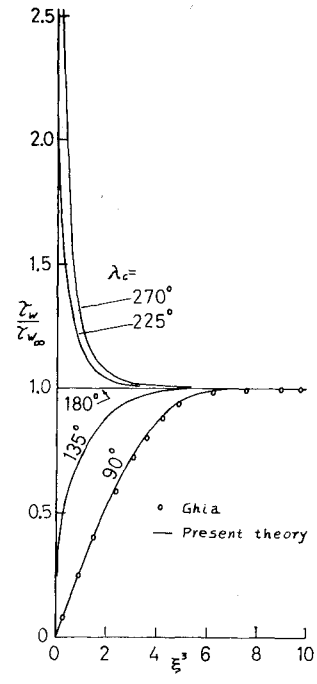

Fig. 12 Variations of wall shear stress with corner angle.

crossflow maps Figs. 10 and 11 drawn for $\lambda_c = 90$ and 270 deg, respectively. In these maps the arrows represent only the direction of the crossflow at the point to which they are attached and not the magnitude.

A point of interest in the crossflow is the negative values of $v^*(2)$ found in and very close to the symmetry plane when $\lambda_c = 270$ deg (Figs. 9 and 11). This behavior was not found in any of the other corners considered. However, it is notable that Ghia's results for the rectangular corner, indicated in Fig. 8, do, in fact, become negative near to the origin, but are of such magnitude as to be hardly discernible on the scale of that figure. For $\lambda_c < 180$ deg a substantial inflow toward the corner along the symmetry plane would have been a stabilizing mechanism for the boundary layer, which in such corners seems to be in a precarious state as a direct consequence of the no-slip boundary condition. In contrast, when $\lambda_c > 180$ deg the boundary layer is not so much in need of such assistance and the appearance of an inflow is, therefore, less important here than it would have been for smaller angles.

C. Wall Shear Stress

The contribution to the wall shear stress from the crossflow velocity is negligible compared with that from the streamwise velocity. Consequently, the wall shear stress τ_w is assumed to be given by

$$\tau_w = \frac{\mu}{\cos\lambda} \frac{\partial v(1)}{\partial x^2}\bigg|_{x^2=0}$$

which, in terms of the corner layer variables, becomes

$$\tau_w = \tau_{w_\infty} \frac{(\partial u/\partial \xi^2)_{\xi^2=0}}{f''(0)}$$

where $\mu = \rho\nu$ and τ_{w_∞} is the value of τ_w at $\xi^3 \to \infty$.

Results for 90 deg $\leq \lambda_c \leq$ 270 deg are shown in Fig. 12 with Ghia's results for the 90 deg corner added for comparison. The two sets of results for the 90 deg case are in close agreement. With regard to the shear stress near the symmetry plane, corners are separable into two groups according as their angle λ_c is greater or less than 180 deg. For $\lambda_c > 180$ deg τ_w rises to rather large values as $\xi^3 \to 0$, but goes to zero in the same limit for $\lambda_c < 180$ deg.

The extent of the corner influence might conveniently be defined as the distance from the symmetry plane $\xi^3 = 0$ to the point where $|1 - \tau_w/\tau_{w\infty}| = 0.01$, and how this point varies with corner angle is evident from Fig. 12.

References

[1] Rubin, S. G., "Incompressible Flow Along a Corner," *Journal of Fluid Mechanics*, Vol. 26, Pt. 1, 1966, pp. 97-110.

[2] Pal. A. and Rubin, S. G., "Asymptotic Features of Viscous Flow Along a Corner," *Quarterly of Applied Mathematics*, Vol. 29, April 1971, pp. 91-108.

[3] Rubin, S. G. and Grossman, B., "Viscous Flow Along a Corner: Numerical Solution of the Corner Layer Equations," *Quarterly of Applied Mathematics*, Vol. 29, July 1971, pp. 169-186.

[4] Desai, S. S. and Mangler, K. W., "Incompressible Laminar Boundary Layer Flow Along a Corner Formed by Two Intersecting Planes," RAE Tech. Rept. 74062, 1974.

[5] Ghia, K. N., "Incompressible Streamwise Flow along an Unbounded Corner," *AIAA Journal*, Vol. 13, July 1975, pp. 902-907.

[6] Ghia, K. N., private communication.

[7] Rosenhead, L. (ed.), *Laminar Boundary Layers*, Clarendon Press, Oxford, 1963, p. 223.